On the motion of thin airfoils in fluids of finite electrical conductivity

By JAMES E. McCUNE
Cornell University, Ithaca, New York†

(Received 29 September 1958 and in revised form 4 May 1959)

A two-dimensional, small-perturbation theory for the steady motion of thin lifting airfoils in an incompressible conducting fluid, with the uniform applied magnetic field perpendicular to (and in the plane of) the undisturbed, uniform flow field, is described. The conductivity of the fluid is assumed to be such that the magnetic Reynolds number, R_m, of the flow is large but finite. Within this assumption, a theory based on superposition of sinusoidal modes is constructed and applied to some simple thin airfoil problems.

It is shown that with this particular field geometry the Alfvén wave mechanism is important in making possible very deep penetration into the flow field of currents and their associated vorticity. It is also shown that the current penetration for an airfoil is much larger than for a wavy wall of wavelength equal to the airfoil chord.

A value of $R_m = 5$ is found to be a good approximation to infinity in this study; in fact, use of the present technique for values of R_m of the order of unity is permissible. These results provide an indication of what is meant by 'large' magnetic Reynolds number in two-dimensional magneto-aerodynamics.

Introduction

In a recent paper Sears & Resler (1959) have developed basic small-perturbation theories for the interaction of the steady two-dimensional motion of an inviscid, incompressible fluid of large conductivity (i.e. large magnetic Reynolds number, R_m) with magnetic fields of two different orientations. They were concerned primarily with the case of infinite R_m; for that case they succeeded in determining the pressure distributions on perfectly insulating sinusoidal walls and thin airfoils when the applied magnetic field is either parallel or perpendicular to (and in the plane of) the undisturbed, uniform flow field. For easy reference we refer to these two orientations as 'aligned' or 'crossed'.

The extensive results obtained by Sears & Resler divide essentially into two parts, depending on the orientation of the applied magnetic field. In the case of aligned fields the basic irrotational flow pattern is unchanged if $R_m = \infty$; the essential new phenomenon is the appearance of surface currents that modify the values of the normal stresses acting on the flow boundaries, whether wavy wall or thin airfoil. These stresses remain in phase with the classical (no magnetic field) surface pressures, and no drag results from the magneto-aerodynamic interaction. When the magnetic Reynolds number is large but finite, on the other hand, the

† Now with Aeronautical Research Associates of Princeton, Inc.

surface currents diffuse into the flow field a distance proportional to $R_m^{-\frac{1}{2}}$ and a boundary layer of current appears. The stresses on the surface are unchanged so long as the 'boundary-layer' approximation holds, and again no drag is predicted. This last result enhances the importance, for aligned fields, of the infinite-conductivity theories.

The important phenomena when the applied magnetic field and undisturbed fluid velocity are mutually perpendicular are markedly different. For infinite R_m standing waves analogous to Mach waves appear, and these waves (which arise from the Alfvén mechanism) carry vorticity and current into the flow field. An important feature of the theory is the appearance of an irrotational elliptic part of the flow field in conjunction with the rotational part arising from the Alfvén mechanism. The pressures on the boundaries are modified from their classical values in the crossed-fields case in such a way that a net drag appears corresponding to the energy carried off by the Alfvén waves. When large but finite values of R_m are introduced, the current and vorticity waves become diffused as they move away from the body. The situation is then analogous to the viscous attenuation of sound waves (Rayleigh 1946; Lighthill 1956) rather than to boundary-layer phenomena.

Sears & Resler have not analysed the finite R_m case for crossed-fields except to show how sinusoidal waves decay. However, the pressures and forces acting on an insulating wavy wall are modified for crossed-fields by the introduction of finite values of R_m (Resler & McCune 1960); so it is important to investigate the extent to which the general infinite R_m theory of Sears & Resler must be modified in this case to allow calculation of significant aerodynamic quantities for finite values of R_m. It is of particular interest to investigate how far into the flow-field current waves actually penetrate for finite bodies (as contrasted with the infinite sinusoidal wall). The results of such a study can be used as a measure of the possible importance, for typical aerodynamic configurations, of electro-magnetic interaction with the flow field.

The present paper presents techniques applicable to linearized, incompressible magneto-aerodynamic problems involving a combination of the phenomena of Alfvén propagation and current diffusion set up by flows past bodies made of perfectly insulating material. The central concern of the paper is with the finite-conductivity magneto-aerodynamic flow fields of cylindrical bodies of finite chord, e.g. thin airfoils, and a procedure using Fourier synthesis of sinusoidal modes (in an approximate form valid for large R_m) is suggested.

As a basis for this approach, the exact sinusoidal solutions of the governing equations are described and relations between the rotational parts of the magnetic and velocity fields are developed for each mode. The solutions given are more general than those of Sears & Resler, since they hold for all R_m, but they are only a special case of more recent results (Resler & McCune 1960) which include effects of compressibility and arbitrary field orientation.

These sinusoidal modes, of course, can be used to obtain the flow past infinite sinusoidal walls; examples have been worked out in detail by Resler & McCune. In order to give a preliminary indication of the range of validity of the present large R_m approximation, exact results for the pressures on an infinite insulating

sinusoidal wall are quoted from the latter work and compared with results obtained for the same problem using the approximate form of the sinusoidal modes.

In the main portion of the paper a theory applicable to flows past thin airfoils, when the magnetic Reynolds number is large but finite, is developed for the crossed-fields configuration. As in the infinite-conductivity case, rotational and irrotational parts of the field appear. The technique used here is to construct the *rotational part* of the field by means of superposition of the appropriate sinusoidal modes and to relate this to the *irrotational part* through the boundary conditions at the insulating body. This procedure leads to the formulation of a boundary-value problem of mixed type (see, for example, equations (35a, b)), which provides the extension of the Sears–Resler theory to finite values of R_m. Both the rotational and irrotational parts of the field are modified for finite R_m.

The method, which is correct to order $(4\pi R_m)^{-1}$, is worked out in the present paper only for the lifting airfoil of zero thickness; the thickness problem can be treated by a completely analogous procedure. The cyclic constant of the elliptic field is determined in this paper by application of the Kutta condition, which requires that the pressure be continuous at the trailing edge of the airfoil.

One of the results of the theory is a practical estimate of the depth of penetration of the current into the flow field for values of R_m of the order of one or greater.

The linearized equations

The governing equations of magneto-aerodynamics have been discussed recently by several authors (see, for example, Cowling (1957) and Resler & Sears (1958)). Our present interest is in the form these equations take for steady, two-dimensional inviscid motion.

Let us denote dimensional quantities by ($\hat{}$). The assumption of two-dimensionality requires that the electric field have only a single component normal to the flow

$$\hat{\mathbf{E}} = (0, 0, \hat{E}), \tag{1}$$

whereas the condition of steady flow requires (Faraday's Law)

$$\operatorname{curl} \hat{\mathbf{E}} = 0. \tag{2}$$

Equations (1) and (2) together imply that $\hat{\mathbf{E}} = \hat{E}\mathbf{k}$ is constant throughout the flow field.

The governing equations can be linearized in accordance with the following conditions. The disturbance-free configuration consists of a uniform electrically conducting incompressible inviscid fluid stream of speed U in the presence of a uniform applied magnetic field of strength H_∞ oriented normal to the free-stream direction in the plane of the flow. In the absence of disturbances it is specified that *no currents flow*, thus implying that the constant value of the electric field is $-UH_\infty$. The electrical conductivity, σ, of the gas is considered a scalar and constant throughout the field, and displacement currents are neglected.

We write the velocity vector $\hat{\mathbf{q}} = (U + \hat{u}, \hat{v}, 0)$ and the magnetic-field vector $\hat{\mathbf{H}} = (\hat{h}_x, H_\infty + \hat{h}_y, 0)$ and assume

$$\frac{\hat{u}}{U}, \frac{\hat{v}}{U} \ll 1 \quad \text{and} \quad \frac{\hat{h}_x}{H_\infty}, \frac{\hat{h}_y}{H_\infty} \ll 1.$$

Under these conditions both the momentum equation and Ohm's Law can be linearized and written in dimensionless form

$$\frac{\partial \mathbf{q}}{\partial x} + \nabla p = \frac{1}{m^2}\left\{\frac{\partial \mathbf{H}}{\partial y} - \nabla h_y\right\}, \tag{3}$$

$$\frac{\xi}{4\pi R_m} = u + h_y, \tag{4}$$

where p is the fluid pressure, ξ denotes the magnitude of curl $\mathbf{H} = (0, 0, \xi)$, and Ampère's Law has been used to replace the current by curl $\mathbf{H}$. Absolute electromagnetic units have been used and a magnetic permeability of unity (non-ferromagnetic materials) assumed throughout.

The dimensionless parameters† $R_m \equiv \sigma U L$ and $m \equiv U\sqrt{(4\pi\rho)}/H_\infty$ are respectively the magnetic Reynolds number and the ratio of the free-stream speed to the Alfvén speed (which might be called the 'magnetic Mach number'). Dimensional quantities, denoted by ($\hat{}$), are obtained from the dimensionless ones through the definitions

$$\left.\begin{aligned} &\hat{p} = \rho U^2 p, \quad \hat{\mathbf{q}} = U\mathbf{q}, \quad (\hat{x}, \hat{y}, \hat{z}) = L(x, y, z), \\ &\hat{\mathbf{H}} = H_\infty \mathbf{H}, \quad \hat{\mathbf{j}} = \sigma U H_\infty \mathbf{j}, \\ &\hat{\boldsymbol{\xi}} \equiv \operatorname{curl} \hat{\mathbf{H}} = \frac{H_\infty}{L} \operatorname{curl} \mathbf{H} \equiv \frac{H_\infty}{L}\boldsymbol{\xi}, \end{aligned}\right\} \tag{5}$$

where ρ is the mass density, $\hat{\mathbf{j}}$ is the current density, and L is some appropriate length for the given problem.

Equation (4) is available in such simple form only in two-dimensional cases where $\hat{\mathbf{E}}$ is constant and known. An alternative expression which is sometimes useful can be obtained by taking the curl of Ohm's Law, thus eliminating $\hat{\mathbf{E}}$ through equation (2). In linearized, dimensionless form the result is

$$\frac{\partial \mathbf{H}}{\partial x} - \frac{\partial \mathbf{q}}{\partial y} = \frac{1}{4\pi R_m} \nabla^2 \mathbf{H}. \tag{6}$$

This relation is correct for any (linearized) steady flow with the crossed-field orientation.

Taking the divergence of (3) yields

$$\nabla^2\left(p + \frac{1}{m^2} h_y\right) = 0 \quad \text{(for any value of } R_m\text{)}, \tag{7}$$

since div $\mathbf{H}$ and div $\mathbf{q}$ are zero. Finally, taking the curls of (3) and (6) and cross-differentiating, one finds (Sears & Resler 1959)

$$\frac{\partial^2 \xi}{\partial x^2} - \frac{1}{m^2}\frac{\partial^2 \xi}{\partial y^2} = \frac{1}{4\pi R_m} \nabla^2 \frac{\partial \xi}{\partial x} \tag{8}$$

and

$$\frac{\partial^2 \Omega}{\partial x^2} - \frac{1}{m^2}\frac{\partial^2 \Omega}{\partial y^2} = \frac{1}{4\pi m^2 R_m} \nabla^2 \frac{\partial \xi}{\partial y}, \tag{9}$$

where Ω is the magnitude of the curl of the velocity field. Note that if $R_m = \infty$, both ξ and Ω obey wave equations.

It is of interest to note that when R_m is large but finite, equation (8) can easily be put into a form analogous with the damped sound-wave equation first studied

† In the absolute e.m.u. system of units the conductivity has purely mechanical dimensions. The R_m defined here differs from that used by some authors by a factor of 4π.

by Stokes and recently analysed further by Lighthill (1956). (In the process, terms of order R_m^{-2} are neglected.) By noting that

$$\nabla^2 \frac{\partial \xi}{\partial x} = \frac{\partial}{\partial x} \nabla^2 \xi \quad \text{and that} \quad \frac{\partial^2 \xi}{\partial x^2} = \frac{1}{m^2} \frac{\partial^2 \xi}{\partial y} + O(R_m^{-1}),$$

we can write (8) in the iterative forms

$$\frac{\partial^2 \xi}{\partial x^2} - \frac{1}{m^2} \frac{\partial^2 \xi}{\partial y^2} \approx \frac{1}{4\pi R_m} (1 + m^{-2}) \frac{\partial^2 \xi}{\partial y^2 \partial x} \tag{10a}$$

$$\approx \frac{1}{4\pi R_m} (1 + m^2) \frac{\partial^3 \xi}{\partial x^3}. \tag{10b}$$

Equation (10*a*) is in the form of Lighthill's equations (31), p. 267.

The basic sinusoidal modes

In this section we shall develop the basic relationships between the sinusoidal modes of the velocity and magnetic fields needed for our subsequent Fourier synthesis method of treating finite-body problems.

Any of equations (8), (10*a*) or (10*b*) can be solved approximately for general flows in exactly the same way as in the treatment given by Lighthill. First, however, we may observe that equation (8) can be solved exactly for an elementary sinusoidal mode, yielding a solution, valid for any value of R_m, which takes the form

$$\xi_\lambda(x, y) = A_\lambda e^{i\lambda x} \exp\left[\mp \lambda m y \sqrt{\left\{ -\left(1 - \frac{i\lambda}{4\pi R_m}\right) \Big/ \left(1 + \frac{i\lambda m^2}{4\pi R_m}\right) \right\}} \right] \tag{11}$$

for $y \gtrless 0$. This expression is useful in making clear the behaviour of a sinusoidal current 'wave' for any value of R_m, large or small. It can in fact be used to construct the flow field for a wavy wall for all R_m (Resler & McCune 1960). We are primarily interested here, however, in the form assumed by equation (11) when R_m is large, since the superposition theory for flows past finite bodies is relatively simple only when the square root in (11) is expanded for either large or small R_m.

When $\lambda(m^2 + 1)/4\pi R_m$ is small compared with one,† the solution (11) takes the approximate form, for $y \gtrless 0$,

$$\xi_\lambda(x, y) \approx A_\lambda e^{i\lambda(x - my)} e^{\mp \lambda^2 \gamma y}, \tag{12}$$

where

$$\gamma \equiv \frac{m(m^2 + 1)}{8\pi R_m}$$

and the boundary condition of no incoming waves has been applied. This result is given by Sears & Resler and is clearly in the form of a damped propagating wave. It is also the approximate solution to either of equations (10*a*) or (10*b*) and is in the form given by Lighthill and others for a damped, plane sound wave.

† Note that this amounts to the specification of a 'cut-off' value for the wave number λ when expansions for large values of R_m are used. Such a restriction on λ arises from the fact that the large R_m approximation depends on the magnetic Reynolds number (based on wavelength) appropriate for each mode being large. This condition must always be violated for some sufficiently high mode, but it is not expected that such violations will lead to any important errors in practical aerodynamic problems (see the later discussion). Throughout this paper the parameter m is taken to be a quantity of order unity, wherever the large R_m approximation is used.

If R_m is based on the wavelength of a sinusoidal wall and λ is taken to correspond to the fundamental mode, then $\lambda = 2\pi$. Such a wave is damped to $1/e$ its value at the wall when y has the value

$$(\lambda^2\gamma)^{-1} = \frac{2R_m}{\pi m(m^2+1)}.$$

This is the damping distance for large R_m, obtained by Sears & Resler, which is appropriate for current waves set up by the motion of a conducting fluid past a sinusoidal wall.

Substitution of (11) into (9), and use of the boundary conditions at $y = \infty$, shows that for $y \geqslant 0$

$$\left.\begin{aligned} \Omega_\lambda(x,y) &= B_\lambda e^{i\lambda x}\exp\left[-\lambda m y\sqrt{\left\{\left(\frac{i\lambda}{4\pi R_m}-1\right)\Big/\left(1+\frac{i\lambda m^2}{4\pi R_m}\right)\right\}}\right] \\ \text{provided}\quad B_\lambda &= +\frac{i\sqrt{\left\{\left(\frac{i\lambda}{4\pi R_m}-1\right)\Big/\left(1+\frac{i\lambda m^2}{4\pi R_m}\right)\right\}}}{m}A_\lambda. \end{aligned}\right\} \tag{13}$$

This provides the essential connexion between the curls of the velocity and magnetic fields. Equations (13) can of course be expanded in an obvious way for large values of R_m, and they then take on a form analogous to equations (12), with

$$B_\lambda \approx -\frac{(m-i\lambda\gamma)}{m^2}A_\lambda. \tag{13a}$$

If we break up the perturbation fields into rotational and irrotational parts

$$\mathbf{v} \equiv (u,v) = \mathbf{v}_R + \nabla\phi_1,$$
$$\mathbf{h} \equiv (h_x,h_y) = \mathbf{h}_R + \nabla\phi_2,$$

and keep in mind that the magnetic and velocity fields are both divergence free, (11) and (13) can be integrated immediately to give the perturbation components in the upper half plane

$$\left.\begin{aligned} u_\lambda &= -\frac{m\sqrt{\left\{\left(\frac{i\lambda}{4\pi R_m}-1\right)\left(1+\frac{i\lambda m^2}{4\pi R_m}\right)\right\}}}{\lambda(1+m^2)}B_\lambda e^{i\lambda x}\exp\left[-\lambda m y\sqrt{\frac{\frac{i\lambda}{4\pi R_m}-1}{1+\frac{i\lambda m^2}{4\pi R_m}}}\right]+\frac{\partial\phi_1}{\partial x}, \\ v_\lambda &= -\frac{i\left(1+\frac{i\lambda m^2}{4\pi R_m}\right)}{\lambda(1+m^2)}B_\lambda e^{i\lambda x}\exp\left[-\lambda m y\sqrt{\frac{\frac{i\lambda}{4\pi R_m}-1}{1+\frac{i\lambda m^2}{4\pi R_m}}}\right]+\frac{\partial\phi_1}{\partial y}, \\ h_{x\lambda} &= -\frac{m\sqrt{\left\{\left(\frac{i\lambda}{4\pi R_m}-1\right)\left(1+\frac{i\lambda m^2}{4\pi R_m}\right)\right\}}}{\lambda(1+m^2)}A_\lambda e^{i\lambda x}\exp\left[-\lambda m y\sqrt{\frac{\frac{i\lambda}{4\pi R_m}-1}{1+\frac{i\lambda m^2}{4\pi R_m}}}\right]+\frac{\partial\phi_2}{\partial x}, \\ h_{y\lambda} &= -\frac{i\left(1+\frac{i\lambda m^2}{4\pi R_m}\right)}{\lambda(1+m^2)}A_\lambda e^{i\lambda x}\exp\left[-\lambda m y\sqrt{\frac{\frac{i\lambda}{4\pi R_m}-1}{1+\frac{i\lambda m^2}{4\pi R_m}}}\right]+\frac{\partial\phi_2}{\partial y}, \end{aligned}\right\} \tag{14}$$

provided $\nabla^2\phi_1 = \nabla^2\phi_2 = 0$. This step is analogous to the procedure used by Sears & Resler and amounts to a definition of the potentials ϕ_1 and ϕ_2.

The rotational parts of the velocity and magnetic fields are related for each mode through equations (13) and (14). The potentials ϕ_1 and ϕ_2 can also be related through the linearized Ohm's Law, equation (4), by observing that equality between rotational and irrotational parts of any equation must hold separately. Thus

$$\frac{\partial\phi_1}{\partial x} = -\frac{\partial\phi_2}{\partial y} \tag{15}$$

for all R_m. Furthermore, differentiation of (15) with respect to x, use of the fact that $\nabla^2\phi_1 = 0$, and subsequent integration with respect to y shows that

$$\frac{\partial\phi_1}{\partial y} = \frac{\partial\phi_2}{\partial x} + f(x) \tag{16}$$

and $f(x) = 0$ because of the boundary condition of uniform flow at $y = \infty$. Equations (15) and (16) are general and hold for any flow field with this field orientation. They were also given by Sears & Resler for $R_m = \infty$.

The wavy wall solution

Before turning to the application of the above results to general flow problems, let us look briefly at the effects of finite conductivity in modifying the forces acting on an infinite, perfectly insulating sinusoidal wall, specified by $Y(x) = \epsilon\cos 2\pi x$. These results (Resler & McCune 1960) are merely quoted here and are intended both as an illustration of the importance of finite conductivity for crossed-fields and as an indication of the error involved in approximating the solutions for large R_m.

Resler & McCune show for the crossed-fields case that the pressure on the surface of the wavy wall is given in general by (real part implied)

$$p(x,0^+) - p_\infty = \frac{-2\pi\epsilon\left[m^2\left(1+m\sqrt{\left\{\left(\frac{i\lambda}{4\pi R_m}-1\right)\Big/\left(1+\frac{i\lambda m^2}{4\pi R_m}\right)\right\}}\right)+2\right]}{m\left[m+(m^2+2)\sqrt{\left\{\left(\frac{i\lambda}{4\pi R_m}-1\right)\Big/\left(1+\frac{i\lambda m^2}{4\pi R_m}\right)\right\}}\right]} e^{2\pi ix} \tag{17}$$

or, for large R_m and m of order unity

$$p(x,0^+) - p_\infty = \frac{-2\pi\epsilon}{m(m-2i)}\left\{m^2 - 2i - 2 + \frac{(m-i)^2}{R_m(m-2i)}\right\} e^{2\pi ix} \tag{18}$$

correct to order R_m^{-1}.

It will be seen that the first term in brackets in (18) is the same as that obtained by Sears & Resler for $R_m = \infty$. The second term represents the first correction to the pressure for finite values of R_m.

A phase diagram comparing the real and imaginary parts of $(p-p_\infty)e^{-2\pi ix}/(-2\pi\epsilon)$ for various values of R_m ranging from 0 to ∞ is presented in figure 1. It will be seen that the effect of finite R_m is to shift the phase in such a way as to decrease the drag per wavelength for any m. In fact, for large R_m the drag per wavelength is given by

$$C_D \equiv \frac{\hat{D}}{\rho U_\infty^2 L} = \frac{4\pi^2\epsilon^2}{m(m^2+4)}\left\{2 - \frac{m(m^2+2)}{R_m(m^2+4)}\right\}. \tag{19}$$

Note that for $m = 1$ and $R_m = 5$ the correction is only 6 %. Expression (19) is plotted against R_m in figure 2 for $m = 1$ and $m = 3$, and compared with the exact result obtained from (17).

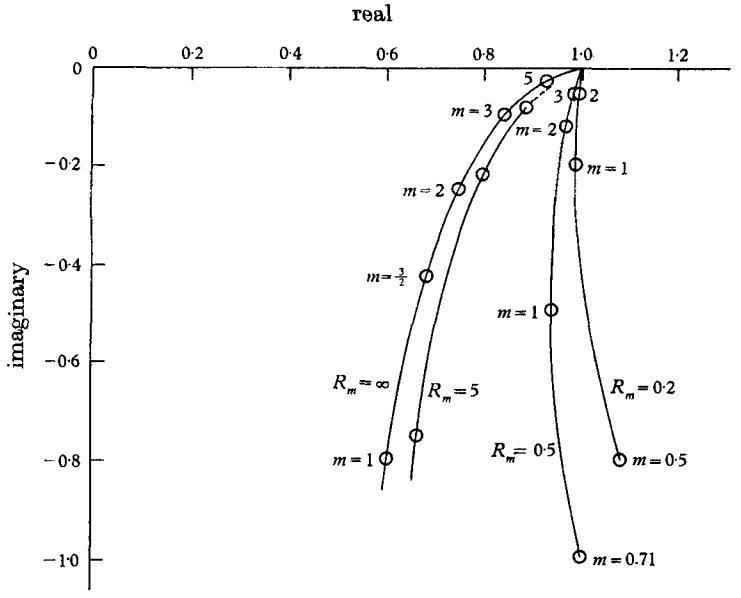

FIGURE 1. Phase diagram showing the pressure on a sinusoidal wall $Y = \epsilon \cos 2\pi x$, for crossed-fields and several values of $R_m (= \sigma UL)$ and $m (= U(4\pi\rho)^{\frac{1}{2}}/H_\infty)$. The diagram gives the real and imaginary parts of the quantity $[p(x, 0^+) - p_\infty]\, e^{-2\pi i x}/(-2\pi\epsilon)$; a negative imaginary part leads to positive drag.

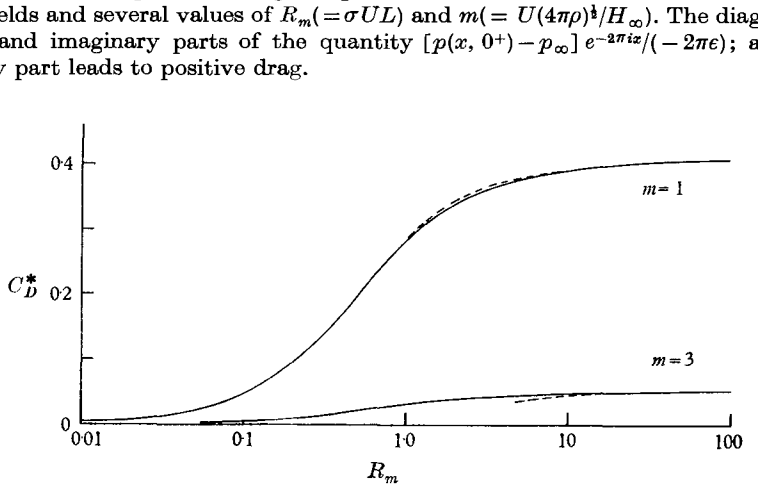

FIGURE 2. Drag per wavelength on the sinusoidal wall of figure 1. The quantity $C_D^* \equiv \hat{D}/(4\pi\rho U_\infty^2 L\epsilon^2)$ is plotted against R_m for the complete (all R_m) theory and compared with the present large R_m approximation. —, all R_m; - - - -, large R_m approximation.

It will be seen from figures 1 and 2 that for this simple case of the flow over a sinusoidal wall, a value of $R_m = 5$ is large enough to provide an acceptable approximation to infinity when m is near one; moreover, the large R_m approximation is successful near $R_m = 1$. We shall see subsequently that this result holds true also for certain typical thin airfoil problems.

Thin-airfoil theory

Use of Fourier synthesis

The results obtained above for sinusoidal modes can be used through Fourier synthesis to provide the basis for solution of any small-perturbation problem. In particular, it is useful to study the flow field associated with a lifting airfoil of small camber moving in a fluid of large but finite conductivity, in order to determine in that case the range of influence of the electro-magnetic body force.

With this in mind, and for the purposes of simplicity, we shall use the above results for the Fourier components in their approximate form for large R_m, correct to order R_m^{-1}. In view of the existence of a finite 'cut-off' value for the wave-number λ (see footnote p. 453) it will be necessary to assume that the airfoils with which we are concerned are so shaped that the higher Fourier components of the induced rotational fields are not too important. In other words, if

$$\xi(x, 0^+) = \int_{-\infty}^{\infty} A^+(\lambda)\, e^{i\lambda x}\, d\lambda \tag{20}$$

we shall generally require $A^+(\lambda)$ to vanish sufficiently strongly as $|\lambda| \to \infty$. This condition will be discussed further in a later section.

We shall introduce the notation y^+ and y^- to denote respectively the upper and lower half planes. Applying the condition that there are no incoming waves, we have from (12) the approximate relations

$$\left.\begin{aligned} \xi(x, y^+) &= \int_{-\infty}^{\infty} A^+(\lambda)\, e^{i\lambda(x-my)} e^{-\lambda^2 \gamma y}\, d\lambda, \\ \xi(x, y^-) &= \int_{-\infty}^{\infty} A^-(\lambda)\, e^{i\lambda(x+my)} e^{+\lambda^2 \gamma y}\, d\lambda. \end{aligned}\right\} \tag{21}$$

These relations can be reduced to an integration over the values of ξ on the x-axis through the use of Fourier inversion. In complete analogy with Lighthill's treatment of damped sound waves, we find

$$\left.\begin{aligned} \xi(x, y^+) &= \frac{1}{m^{\frac{1}{2}} \sqrt{\left(\frac{1}{2R_m}(1+m^{-2})\, y\right)}} \int_{-\infty}^{\infty} \xi(u, 0^+) \exp\left[-\frac{\left(\frac{x-u}{m} - y\right)^2}{\frac{m}{2\pi R_m}(1+m^{-2})\, y} \right] du, \\ \xi(x, y^-) &= \frac{1}{m^{\frac{1}{2}} \sqrt{\left(\frac{-1}{2R_m}(1+m^{-2})\, y\right)}} \int_{-\infty}^{\infty} \xi(u, 0^+) \exp\left[+\frac{\left(\frac{x-u}{m} - y\right)^2}{\frac{m}{2\pi R_m}(1+m^{-2})\, y} \right] du. \end{aligned}\right\} \tag{22}$$

Thus, if the current density on the x-axis is known or can be determined, it is determined throughout the field.

Moreover, because the Fourier components of the *rotational parts* on the fields (u_R, v_R, h_{xR}, h_{yR}, as well as Ω and ξ) all have the same functional form, each quantity can be written for the upper and lower half planes exactly as in (22) with $\xi(u, 0)$ replaced in each case by the values of the quantity in question on the x-axis. Also, the Fourier transform of each rotational quantity can be related to

the Fourier transform of any other rotational quantity just as B_λ and A_λ were related in equation (13a). Consequently, knowledge of any one of the rotational quantities on the x-axis will determine all the others everywhere. We shall treat $v_R(x, 0^\pm)$ as the important quantity, because of its close connexion with the usual aerodynamic boundary condition at the airfoil.

The relations between the various Fourier transforms follow in a straightforward manner from the approximate form of equations (13) and (14) and their counterparts for $y < 0$. If we pair the functions and their transforms as indicated in table 1, then each of the functions listed obeys an equation like (20). Some of the important relations between the transforms that follow approximately from (13) and (14) are given in table 2, correct to order

$$\gamma = \frac{m(m^2+1)}{8\pi R_m}.$$

Function	$\xi(x, 0^\pm)$	$\Omega(x, 0^\pm)$	$h_{xR}(x, 0^\pm)$	$h_{yR}(x, 0^\pm)$	$u_R(x, 0^\pm)$	$v_R(x, 0^\pm)$
Transform	$A^\pm(\lambda)$	$B^\pm(\lambda)$	$C^\pm(\lambda)$	$D^\pm(\lambda)$	$E^\pm(\lambda)$	$F^\pm(\lambda)$

TABLE 1

$B^\pm(\lambda) = \mp \frac{(m - i\lambda\gamma)}{m^2} A^\pm(\lambda)$	(2.1)	$A^\pm(\lambda) = \mp m \left[i\lambda(1+m^2) - \frac{\lambda^2\gamma}{m}(1-m^2) \right] F^\pm(\lambda)$	(2.6)
$B^\pm(\lambda) = [i\lambda(1+m^2) + 2\lambda^2 m\gamma] F^\pm(\lambda)$	(2.2)	$D^\pm(\lambda) = \mp m \left(1 + \frac{i\lambda\gamma}{m}\right) F^\pm(\lambda)$	(2.7)
$E^\pm(\lambda) = \pm (m - i\lambda\gamma) F^\pm(\lambda)$	(2.3)	$C^\pm(\lambda) = -m^2 F^\pm(\lambda)$	(2.8)
$A^\pm(\lambda) = [i\lambda(1+m^2) + 2\lambda^2 m\gamma] D^\pm(\lambda)$	(2.4)	$C^\pm(\lambda) = \mp m \left(1 + \frac{i\lambda\gamma}{m}\right) E^\pm(\lambda)$	(2.9)
$C^\pm(\lambda) = \pm (m - i\lambda\gamma) D^\pm(\lambda)$	(2.5)	$D^\pm(\lambda) = -m \left(1 + \frac{2i\lambda\gamma}{m}\right) E^\pm(\lambda)$	(2.10)

TABLE 2

These results imply, for example, that

$$h_{xR}(x, 0^\pm) = -m^2 v_R(x, 0^\pm), \tag{23}$$

$$h_{yR}(x, 0^\pm) = \mp m \left[v_R(x, 0^\pm) + \frac{\gamma}{m} v_R'(x, 0^\pm) \right], \tag{24}$$

$$\xi(x, 0^\pm) = \mp m \left[(1+m^2) v_R'(x, 0^\pm) + \frac{\gamma}{m}(1-m^2) v_R''(x, 0^\pm) \right], \tag{25}$$

where the primes denote differentiation with respect to x at $y = 0^\pm$. Note that the symmetry properties of, say, v_R determine the symmetry properties of all the other rotational quantities.

Application of boundary conditions

We are now in a position to apply the boundary conditions appropriate to thin airfoils. For lifting airfoils of small camber and zero thickness we have as usual

$$v(x, 0^{\pm}) = Y'(x) = v_R(x, 0^{\pm}) + \left.\frac{\partial \phi_1}{\partial y}\right|_{y=0^{\pm}}$$

for
$$-\frac{c}{2L} \leqslant x \leqslant \frac{c}{2L}, \tag{26}$$

where c is the chord of the airfoil. We have further the conditions that both h_x and h_y must be continuous at $y = 0$†. Thus

$$h_{yR}(x, 0^+) - h_{yR}(x, 0^-) = -\left[\left.\frac{\partial \phi_2}{\partial y}\right|_{y=0^+} - \left.\frac{\partial \phi_2}{\partial y}\right|_{y=0^-}\right], \tag{27}$$

$$h_{xR}(x, 0^+) - h_{xR}(x, 0^-) = -\left[\left.\frac{\partial \phi_2}{\partial x}\right|_{y=0^+} - \left.\frac{\partial \phi_2}{\partial y}\right|_{y=0^-}\right]. \tag{28}$$

Substituting equation (23) into (28) we find

$$-m^2[v_R(x, 0^+) - v_R(x, 0^-)] = -\left[\left.\frac{\partial \phi_2}{\partial x}\right|_{y=0^+} - \left.\frac{\partial \phi_2}{\partial x}\right|_{y=0^-}\right] \tag{29}$$

Function	Symmetry in y	Function	Symmetry in y
v_R	Symm.	h_{yR}	Antisymm.
Ω	Symm.	u_R	Antisymm.
ξ	Antisymm.	ϕ_1	Antisymm.
h_{xR}	Symm.	ϕ_2	Symm.

TABLE 3

which, with (26), gives for all x

$$m^2\left[\left.\frac{\partial \phi_1}{\partial y}\right|_{y=0^+} - \left.\frac{\partial \phi_1}{\partial y}\right|_{y=0^-}\right] = -\left[\left.\frac{\partial \phi_2}{\partial x}\right|_{y=0^+} - \left.\frac{\partial \phi_2}{\partial x}\right|_{y=0^-}\right]. \tag{30}$$

Comparison of (30) with (16) shows that for all R_m

$$\left.\frac{\partial \phi_1}{\partial y}\right|_{y=0^+} - \left.\frac{\partial \phi_1}{\partial y}\right|_{y=0^-} = 0 \tag{31}$$

and consequently both v_R and $\partial \phi_2/\partial x$ are also continuous at $y = 0$. These results completely determine the symmetry of the problem; for example, the potential part of the flow field arises at most from a distribution of vortices over the airfoil, while the potential part of the magnetic field is due to a (fictitious) distribution of magnetic 'sources and sinks'. The symmetry is thus the same as found by Sears & Resler for $R_m = \infty$. The symmetry properties of the various quantities are listed in table 3.

Further information can be obtained by substituting (27) into Ohm's Law, equation (4): $u(x, 0^+) - u(x, 0^-) = (\xi(x, 0^+) - \xi(x, 0^-))/4\pi R_m$.

† No surface currents can exist, of course, for finite R_m in the steady state, since all currents tend to diffuse away from the boundaries. They do not exist, however, with the present field orientation, even in the limit of $R_m \to \infty$ (Sears & Resler 1959).

But in view of the symmetry properties listed in table 3 this implies

$$u(x, 0^{\pm}) = \frac{\xi(x, 0^{\pm})}{4\pi R_m}, \tag{32}$$

and also

$$h_y(x, 0^{+}) = 0 = h_y(x, 0^{-}). \tag{33}$$

The boundary-value problem for the potential flow

Equation (2.3) of table 2 implies $u_R(x, 0^{\pm}) = \pm m v_R(x, 0^{\pm}) \mp \gamma v_R'(x, 0^{\pm})$ and this result with (25) in (32) leads to a relation between $\partial\phi_1/\partial x|_{y=0^+}$ and $v_R(x, 0)$

$$\begin{aligned}\left.\frac{\partial\phi_1}{\partial x}\right|_{y=0^+} &= -\frac{m(m^2+1)}{4\pi R_m} v_R'(x, 0) - m v_R(x, 0) + \frac{m(m^2+1)}{8\pi R_m} v_R'(x, 0) \\ &= -m v_R(x, 0) - \gamma v_R'(x, 0)\end{aligned} \tag{34}$$

correct to order R_m^{-1}. Eliminating v_R with (26) and iterating in the resulting formula, one easily finds the alternative relations

$$\left.\frac{\partial\phi_1}{\partial x}\right|_{y=0^+} = m \left.\frac{\partial\phi_1}{\partial y}\right|_{y=0^+} - m Y'(x) + \gamma \left.\frac{\partial^2\phi_1}{\partial y\, \partial x}\right|_{y=0^+} - \gamma Y''(x) + O(\gamma^2), \tag{35a}$$

$$\left.\frac{\partial\phi_1}{\partial x}\right|_{y=0^+} = m \left.\frac{\partial\phi_1}{\partial y}\right| - m Y'(x) + \frac{\gamma}{m} \left.\frac{\partial^2\phi_1}{\partial x^2}\right|_{y=0^+} + O(\gamma^2) \tag{35b}$$

for

$$-\frac{c}{2L} \leqslant x \leqslant \frac{c}{2L},$$

either of which provides the necessary boundary conditions for the potential field when added to conditions of vanishing perturbations at infinity and the symmetry properties already determined. It will be seen later that while (35*b*) appears to be in a nicer form it is probably not uniformly valid. For most purposes (35*a*) will be more useful than (35*b*).

The first two terms in the right-hand side of equations (35) will be recognized as forming the potential-flow boundary condition for the infinite R_m case previously determined by Sears & Resler. The last terms in equation (35*a*) represent the first correction of the boundary condition for ϕ_1 due to the fact that R_m is finite. Thus, not only is the rotational part of the field modified when R_m is finite, but also the irrotational field is changed through the boundary condition.

Solution of the potential problem leads to a complete determination of the flow field (within the limitations already stated) since knowledge of $\partial\phi_1/\partial y$ determines v_R on the airfoil through the boundary condition (26). Moreover, v_R is zero off the airfoil (on the x-axis), as can be seen in the following manner: using the results of table 2 with equation (32), we can integrate the x-component of equation (3) on the x-axis to obtain

$$p(x, 0^{\pm}) - p_\infty = -\frac{m^2+1}{m^2} h_{yR}(x, 0^{\pm}) = \pm\frac{(m^2+1)}{m} v_R(x, 0) \pm \frac{\gamma}{m^2}(m^2+1) v_R'(x, 0) \tag{36}$$

correct to order R_m^{-1}. But the pressure perturbations must vanish on the x-axis off the airfoil from symmetry considerations, so $h_{yR}(x, 0^{\pm})$ and its derivatives must vanish off the airfoil. Furthermore, equation (2.7) of table 2 shows that

$$v_R(x, 0) = \mp\frac{1}{m} h_{yR}(x, 0^{\pm}) \pm \frac{\gamma}{m^2} h_{yR}'(x, 0^{\pm}) \tag{37}$$

again correct to R_m^{-1}. Consequently, v_R is known on the entire x-axis, and all rotational quantities, including the currents, are determined, once ϕ_1 is determined.

In addition, the pressure on the boundaries is immediately determined upon solution of the potential problem, since comparison of equations (36) and (34) shows that

$$p(x, 0^{\pm}) - p_\infty = -\frac{m^2+1}{m^2}\frac{\partial \phi_1}{\partial x}\bigg|_{y=0^{\pm}}, \tag{38}$$

which also implies that

$$h_{yR}(x, 0^{\pm}) = \frac{\partial \phi_1}{\partial x}\bigg|_{y=0^{\pm}}. \tag{39}$$

This last relation determines $\partial\phi_2/\partial y|_{y=0^{\pm}}$, in view of equation (33).

Note, finally, that the Kutta condition is satisfied, through equation (38), provided only that $\partial\phi_1/\partial x|_{y=0^+}$ is finite at the trailing edge.

Application to thin airfoils

(*a*) *Direct problem*

The potential-flow boundary condition (35*a*) presents a rather formidable boundary-value problem when only $Y'(x)$ is given, since it amounts to a differential equation relating potential derivatives of different order on the airfoil. For example, the solution due to Rott & Cheng (1954), available when $R_m = \infty$, no longer applies.

The theory of conjugate functions enables one to write (35*a*) as an integro-differential equation in $\partial\phi_1/\partial y|_{y=0^+}$

$$m\frac{\partial \phi_1}{\partial y}\bigg|_{y=0^+} = \frac{1}{\pi}\sqrt{\left(\frac{(c/2L)-x}{(c/2L)+x}\right)}\,\mathscr{P}\int_{-c/2L}^{c/2L}\frac{\partial \phi_1}{\partial y}\bigg|_{y=0^+}\sqrt{\left(\frac{(c/2L)+\zeta}{(c/2L)-\zeta}\right)}\frac{d\zeta}{x-\zeta} + mY'(x) - \gamma\frac{\partial}{\partial x}\left[\frac{\partial \phi_1}{\partial y}\bigg|_{y=0^+}\right] + \gamma Y''(x) \tag{40}$$

in which the Kutta condition has been applied. The symbol $\mathscr{P}$ denotes the Cauchy principal value. Solution of equation (40) is beyond the scope of the present paper and will be left for future research.

Another approach to the problem, which is somewhat more revealing at this early stage, is to use the Glauert series (Glauert 1926) appropriate for that family of flows wherein

$$\frac{\partial \phi_1}{\partial y}\bigg|_{y=0^+} = -\sum_{n=0}^{\infty} B_n \cos n\theta; \quad \frac{2Lx}{c} = \cos\theta. \tag{41}$$

The Glauert theory shows that in such cases

$$\frac{\partial \phi_1}{\partial x}\bigg|_{y=0^+} = B_0\frac{1-\cos\theta}{\sin\theta} + \sum_{n=1}^{\infty} B_n \sin n\theta \tag{42}$$

and it can be seen that this satisfies the Kutta condition at the trailing edge. Moreover, because of equation (38), the loading is

$$l(x) \equiv -4(p(x, 0^+) - p_\infty) = \frac{4(m^2+1)}{m^2}\frac{\partial \phi_1}{\partial x}\bigg|_{y=0^+} = \frac{4(m^2+1)}{m^2}\left(B_0\frac{1-\cos\theta}{\sin\theta} + \sum_{n=1}^{\infty} B_n \sin n\theta\right) \tag{43}$$

and the lift coefficient becomes

$$C_l = \frac{\text{lift per unit span}}{\frac{1}{2}\rho U_\infty^2 c} = 2\pi\left(\frac{m^2+1}{m^2}\right)\{B_0 + \tfrac{1}{2}B_1\}. \tag{44}$$

It should be noted that the limit $m \to \infty$ gives the classical formula.

Unfortunately, these simple results cannot be taken too seriously, since the profile shapes that correspond to this family of solutions are quite unusual. The condition (35a) implies in this case that

$$Y'(x) + \frac{\gamma}{m} Y''(x) = -\frac{B_0}{m}\left\{\frac{1-\cos\theta}{\sin\theta} + m\right\} - \sum_{n=1}^{\infty} B_n \left\{\cos n\theta + \frac{1}{m}\sin n\theta + \frac{2L\gamma}{cm} n \frac{\sin n\theta}{\sin\theta}\right\}. \tag{45}$$

The profiles corresponding to (45) have singular slopes at the leading edge and singular curvatures at the leading and trailing edges, unless B_0 vanishes. Such geometrical details appear to be necessary in order to set up the family of flows satisfying the Glauert relations, but it is unlikely that real fluids, acting in the presence of boundary layers and unable to respond to detailed profile contours, would actually show the kind of behaviour indicated in (42).

It should be mentioned here that application of (35b) in replacing either (40) or (45) will result in generally more severe singularities at the leading edge (either in the flow field or in the profile shape) than those present when $R_m = \infty$. The iterative procedure used in obtaining (35b) from (35a) is consequently not uniformly valid and should be applied only with great care.

(*b*) *Indirect problem*

Equation (45) illustrates that even the indirect problem of aerodynamics, wherein the pressure is specified and the profile shape is required, is not necessarily simple. Specification of the pressure amounts to specification of $\partial\phi_1/\partial x|_{y=0^+}$ (equation (38)), and from this $\partial\phi_1/\partial y|_{y=0^+}$ can immediately be determined from the familiar relation

$$\left.\frac{\partial\phi_1}{\partial y}\right|_{y=0^+} = -\frac{1}{\pi}\mathscr{P}\int_{-c/2L}^{c/2L} \left.\frac{\partial\phi_1}{\partial x}\right|_{y=0^+} \frac{d\zeta}{x-\zeta}. \tag{46}$$

If $\partial\phi_1/\partial x|_{y=0^+}$ is not singular, this relation, along with the specified value of $\partial\phi_1/\partial x|_{y=0^+}$, can be substituted into (35b) to determine $Y'(x)$. If $\partial\phi_1/\partial x|_{y=0^+}$ is singular, (35a) must be used.

A simple example of the indirect problem for $R_m = \infty$ was given by Sears & Resler. They specified that the loading be elliptic (proportional to $\sin\theta$) and determined the corresponding profile shape. As an example of the use of the present theory, we may repeat their procedure for finite values of R_m.

If the loading is elliptic, only B_1 in the Glauert series is non-zero. Then (45) becomes

$$Y'(x) + \frac{\gamma}{m} Y''(x) = -B_1\left\{\cos\theta + \frac{1}{m}\sin\theta + \frac{2L\gamma}{mc}\right\}. \tag{47}$$

Hence

$$Y(x) = -B_1\left\{(x^2 - \tfrac{1}{4}) + \frac{x}{2m}\sqrt{(1-4x^2)} - \frac{1}{4m}\cos^{-1}2x - \frac{\gamma}{m^2}\sqrt{(1-4x^2)}\right\}, \tag{48}$$

where L has been identified with the airfoil chord, c, and the value of $Y(\frac{1}{2})$ has arbitrarily been put equal to zero. This airfoil shape has been plotted in figure 3 for several values of m and R_m, under the restriction that the magnitude of the loading be the same for each case.

The airfoil shapes shown in figure 3 for $m < \infty$ amount to airfoils of small camber at an angle of attack. The effect of the magnetic field, therefore, is to change the pressure distribution for a given airfoil from essentially that of a flat plate (with leading-edge singularity) to a case of 'shockless entry' with symmetrical loading. Consequently, the magnetic field has a strong (generally

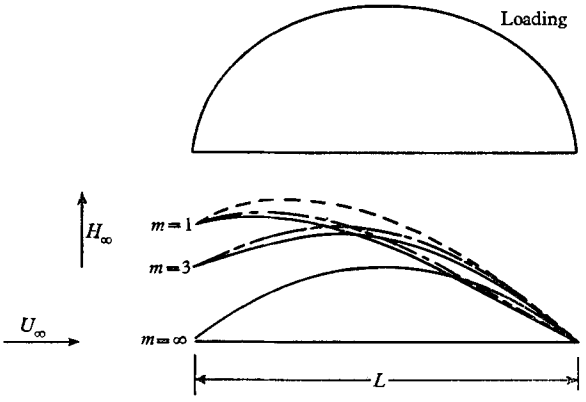

FIGURE 3. Airfoil camber lines producing an elliptic loading for various values of R_m and m. $m=\infty$ gives the classical result for all R_m; the curve $R_m = 1$ is included only for the case $m = 1$. The comparison is made for the same magnitude of the loading (cf. equation (43)). —, $R_m=\infty$ (Sears & Resler 1959); - - - - $R_m = 1$; —·—·—, $R_m = 5$. $R_m=\sigma U_\infty L$.

favourable) effect on the boundary layer and provides a means of shifting the centre of pressure. However, it is clear that except for $m = \infty$ (zero magnetic-field strength) each airfoil is associated with a positive drag. This drag arises from wave energy carried away by the Alfvén mechanism; the effect of finite conductivity is to reduce the drag for the same loading.

It will again be noted, for $m = 1$, that $R_m = 5$ provides a good approximation to the results obtained by Sears & Resler at $R_m = \infty$. This conclusion holds for a wide range of m and is important in defining what we mean by large or infinite magnetic Reynolds numbers.

Current penetration

In order to determine the extent of the important magneto-aerodynamic interaction for an airfoil, let us use the present theory to compute the depth of penetration into the field of the current density. For this purpose, we choose a convenient form for the pressure distribution and use it, through equations (36) and (2.4), to determine a corresponding value of the current density on the airfoil. This will provide sufficient information, through equations (21) or (22), to determine approximately the current penetration into the field.

As an example, let us suppose that on the airfoil

$$p(x, 0^+) - p_\infty = P(1 - 4x^2) = -\frac{m^2+1}{m^2} h_{yR}(x, 0^+), \tag{49}$$

so that

$$\xi(x, 0^+) \approx (1+m^2) h'_{yR}(x, 0^+) = 8m^2 P x. \tag{50}$$

Thus,

$$\xi(x, y^+) \approx \frac{2\xi(\frac{1}{2}, 0^+)}{m^{\frac{3}{2}} \sqrt{\left(\frac{m^2+1}{2m^2 R_m} y\right)}} \int_{-\frac{1}{2}}^{\frac{1}{2}} u\, du \exp\left\{ -\frac{(x - my - u)^2}{\frac{m(m^2+1)}{2\pi R_m} y} \right\} \tag{51}$$

from which it is easily recognized that the limit $R \to \infty$ is $2\xi(\frac{1}{2}, 0^+)(x - my)$, in agreement with Sears & Resler. Further, the right-hand side of equation (51) can be integrated exactly to give

$$\xi(x, y^+) \approx \xi(\tfrac{1}{2}, 0^+) \left\{ \sqrt{\frac{Ky}{\pi}} \left[\exp\left\{ -\frac{(my - x + \frac{1}{2})^2}{Ky} \right\} - \exp\left\{ -\frac{(my - x - \frac{1}{2})^2}{Ky} \right\} \right] \right.$$
$$\left. + (x - my) \left[\operatorname{erf}\left(\frac{\frac{1}{2} + my - x}{\sqrt{Ky}} \right) - \operatorname{erf}\left(\frac{-\frac{1}{2} + my - x}{\sqrt{Ky}} \right) \right] \right\}, \tag{52}$$

where

$$K \equiv \frac{m(m^2+1)}{2\pi R_m} = 4\gamma.$$

This expression has all the correct limits, since

$$\operatorname{erf}(x) \equiv \frac{2}{\sqrt{\pi}} \int_0^x e^{-t^2} dt \quad \text{and} \quad \operatorname{erf}(-\infty) = -\operatorname{erf}(\infty).$$

The distance in chord lengths (measured along the characteristic line $x - my = \frac{1}{2}$) for the current density to fall off to one-tenth its value at $y = 0^+$ is plotted versus R_m in figure 4. The current penetration is infinite if $R_m = \infty$ and still very large for finite R_m.

It is of interest that the current penetration is very much larger for the airfoil in question than for the wavy wall with a wavelength equal to the airfoil chord. In fact, it is easy to check that the sinusoidal mode that is damped by the same ratio at the same height has a wavelength equal to about twenty-five chords. This is related to the fact that the current waves set up by the airfoil diffuse outward from their characteristic lines at the same time that they diminish in intensity, so that an observer at a large height above the airfoil will measure appreciable current density for many chord lengths in the x-direction (see figure 4).

The appearance of the Alfvén mechanism, with its ability to carry currents and the associated vorticity deeply into the flow, renders the crossed-fields case more interesting than it might otherwise be. The large current penetration is in sharp contrast with the aligned-fields case (Sears & Resler 1959), where the Alfvén mechanism cannot penetrate the flow field, and with the small R_m case, where the Alfvén mechanism is not discernible for any field orientation. (In the latter case, the first-order currents are given directly by the fluid motion and the *applied* magnetic field, with the usual hydrodynamic flow pattern prevailing, and consequently the currents die out in about one chord length.)

The large R_m approximation—discussion of error

As mentioned previously, the large R_m approximation, when used in the context of Fourier synthesis, requires the special assumption that the higher harmonics of the rotational part of the flow field (and of the magnetic field) are not too important. It would be useful, therefore, to give an indication of how

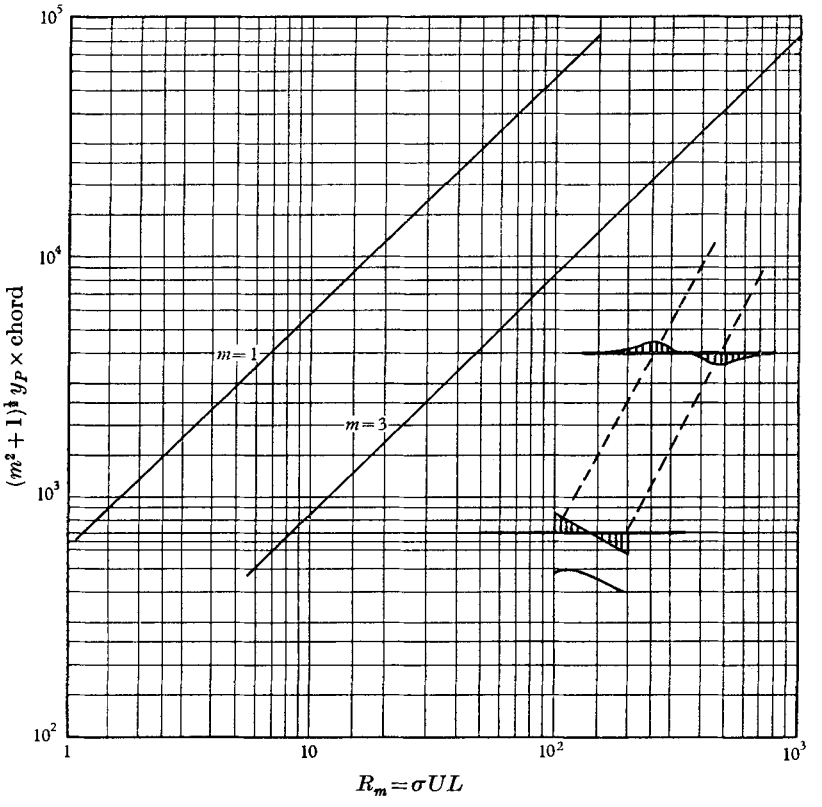

FIGURE 4. Current penetration into the flow field resulting from the Alfvén wave mechanism. The quantity $y_p(m^2+1)^{\frac{1}{2}}$ is the distance in chords, measured along characteristic lines, for the current density to fall off to 0·1 times its value at the airfoil. The inset figure illustrates the chordwise spread, as well as the decay in amplitude, of the current density generated by an airfoil of the shape shown.

rapidly the Fourier transforms occurring in any given problem should fall off for large $|\lambda|$. Any such indication will naturally suffer from a certain degree of arbitrariness, but it is hoped that the discussion given below will, nevertheless, be helpful.

We have at our disposal a clearly defined 'cut-off' value for the wave-number, $\lambda^* = 4\pi R_m/(m^2+1)$, with m explicitly assumed to be of order one. We shall consider the contribution of the Fourier transform for values of λ less than λ^* as an indication of the magnitude of a given quantity. We shall then require that the contribution made for values of λ greater than λ^* be

negligible in comparison with this magnitude. For this purpose we define in the upper half plane

$$\left.\begin{aligned} M &\equiv \int_0^{\lambda^*} F(\lambda)\, e^{i\lambda x} \exp\left[-\lambda m y \sqrt{\left\{\left(\frac{i\lambda}{4\pi R_m} - 1\right) \Big/ \left(1 + \frac{i\lambda m^2}{4\pi R_m}\right)\right\}}\right] d\lambda, \\ \epsilon_T &\equiv \int_{\lambda^*}^{\infty} F(\lambda)\, e^{i\lambda x} \exp\left[-\lambda m y \sqrt{\left\{\left(\frac{i\lambda}{4\pi R_m} - 1\right) \Big/ \left(1 + \frac{i\lambda m^2}{4\pi R_m}\right)\right\}}\right] d\lambda. \end{aligned}\right\} \tag{53}$$

In this approach to the problem there are really two independent considerations that arise. The first has to do simply with the convergence of the Fourier integrals involved. This is a standard problem and has nothing directly to do with the large R_m approximation itself. In order to simplify the following discussion we shall assume that we are dealing with a problem in which the most slowly convergent transforms (see table 2) are absolutely convergent.†

Since the large R_m approximation was introduced in this problem primarily to enable us to deduce the boundary conditions on the x-axis, our first concern is with the behaviour of ϵ_T and M as $y \to 0$. Under the assumption of absolute convergence it will generally be sufficient for the purposes of the large R_m approximation to require that the transform ($F(\lambda)$, say) has no maxima at values of λ greater than λ^* and that $|F(\lambda^*)| \ll |F(\lambda_0)|$, where λ_0 is some reference wave-number at which $|F|$ is at a maximum. To give a specific example, let us suppose that we have a transform of the form $A/[1+(\lambda/\lambda_c)^n]$. In order for this to be absolutely convergent, $n > 1$, and hence $|F(\lambda^*)| \ll |F(0)|$ provided $\lambda^*/\lambda_c \gg 1$. For this example, at the point $x = 0$, $y = 0$, where the effect of the higher harmonics is greatest, we find the ratio of ϵ_T to M to be of the order

$$(\lambda_c/\lambda^*)^{n-1}.$$

Thus, in this example we simply require $\lambda^* \gg \lambda_c$.

Considerations similar to this can be applied for any given problem at $y = 0$ when the boundary conditions are given and the nature of the pertinent transforms has been determined. Often, however, since the value of the function itself will be known on the x-axis, only the behaviour of its transform for wave-numbers greater than λ^* need be determined so that ϵ_T can be compared directly with the function in that region.

It is also of interest to investigate the influence of the higher harmonics on the flow field as a whole, and in particular their comparative importance in the far field. For this purpose we note that, since $\lambda^* = m/2\gamma$,

$$\left.\begin{aligned} |M| &\geqslant \left| \int_0^{m/2\gamma} F(\lambda)\, e^{i\lambda(x-my)} \exp\left(-\frac{\lambda m y}{\sqrt{2}}\right) d\lambda \right|, \\ \epsilon_T &\leqslant \int_{m/2\gamma}^{\infty} |F(\lambda)|\, e^{-\lambda y}\, d\lambda \end{aligned}\right\} \tag{54}$$

† Of course, in practical problems it is not necessary that the Fourier integrals all be absolutely convergent; convergence *in the mean* is sufficient. However, in that case the discussion of the error associated with the large R_m approximation becomes more complicated. For example, ϵ_T does not exist at the point $x = 0$, $y = 0$ unless absolute convergence is assumed. The present discussion is limited to the assumption of absolute convergence for simplicity.

and hence

$$\frac{|\epsilon_T|}{|M|} \leqslant \frac{\int_{m/2\gamma}^{\infty} |F(\lambda)|\, e^{-\lambda y}\, dy}{\left| \int_0^{m/2\gamma} F(\lambda)\, e^{i\lambda(x-my)} \exp\left(-\frac{\lambda m y}{\sqrt{2}}\right) dy \right|} \equiv \mathscr{R}. \tag{55}$$

This is not the closest upper bound that might be constructed, but it has the advantage of being relatively easy to use.

For example, if we again consider Fourier transforms of the form $A/[1+(\lambda/\lambda_c)^n]$, the upper bound of the ratio given by (55) is of the order (for integer n and y not near zero)

$$\mathscr{R} \approx \frac{[(x-my)^2+\frac{1}{2}(m^2y^2)]}{\lambda_c^{-n}(n-1)!} \times \frac{y^{n-1}\, E(\lambda^* y)}{\{[(my/\sqrt{2})\,(1-e^{-ay}\cos\lambda^*\bar{x})+\bar{x}\,e^{-ay}\sin\lambda^* x]^2 + [\bar{x}(1-e^{ay}\cos\lambda^*\bar{x})-(my/\sqrt{2})\,e^{-ay}\sin\lambda^*\bar{x}]^2\}^{\frac{1}{2}}}, \tag{56}$$

where $a = (m^2\sqrt{2}/4\gamma)$, $\bar{x} = (x-my)$ and $E(u)$ is the exponential integral,

$$E(u) \equiv \int_u^{\infty} \frac{e^{-t}\, dt}{t}.$$

It will be noted that $\mathscr{R}$ approaches zero exponentially as $y \to \infty$ for all n, and for any finite value of y it vanishes as $R_m \to \infty$. In particular, if $m = 1$, and $R_m = 3/\pi$, $\mathscr{R}$ is proportional to $e^{-6}/6(n-1)!$ at $y = 1$. Thus, at finite values of y the higher harmonics are automatically damped out rapidly due to the very nature of the rotational parts of the solution, and the large R_m approximation is good in the far field even for functions whose transforms are themselves rather slowly convergent.

Conclusions

We have shown that it is possible to compute, with the assumption that the magnetic Reynolds number R_m is large but finite, significant magneto-aerodynamic quantities for finite bodies immersed in an incompressible fluid stream in the presence of a uniform magnetic field which is perpendicular to the free stream and in the plane of the flow. To do this, the results of an exact calculation of the flow field of a small-amplitude wavy wall, valid for all R_m and m, have been used in approximate form to construct a thin airfoil theory for fluids of large but finite conductivity. The boundary-value problem for the irrotational part of the flow field has been determined, and the method for obtaining the pressure distribution on the airfoil and all rotational parts of the flow field once the boundary-value problem is solved has been given.

We have used the theory to solve the indirect problem of determining the airfoil shape associated with a given loading and have compared the results with those of Sears & Resler for $R_m = \infty$. In addition, we have studied for a particular example the depth of penetration into the flow field of the currents set up by the motion of an airfoil. As shown in figure 4, the depth of penetration of this current,

which is carried into the flow field by the Alfvén mechanism, is surprisingly large. Indeed, it is so large as to emphasize the need for further study of current penetration in practical cases, for example, when the magnetic field is non-uniform, or of finite extent.

Perhaps the most significant conclusion to be drawn from the present study is that a value of $R_m = 5$ is, in the cases studied, large enough to be a good approximation to infinity. Moreover, if the Fourier transforms of the pertinent quantities converge sufficiently rapidly, the present technique of expanding in reciprocal powers of R_m appears to be valid in the neighbourhood of $R_m = 1$. These results help to define what we mean by large magnetic Reynolds number in this area of magneto-aerodynamics.

REFERENCES

COWLING, T. G. 1957 *Magnetohydrodynamics*. London: Interscience.

GLAUERT, H. 1926 *Aerofoil and Airscrew Theory*. Cambridge University Press.

LIGHTHILL, M. J. 1956 *Surveys in Mechanics* (ed. G. K. Batchelor and R. M. Davies). Cambridge University Press.

RAYLEIGH, LORD 1946 *Theory of Sound II*, 2nd ed. New York: Dover.

RESLER, E. L., JR. & MCCUNE, J. E. 1960 *Rev. Mod. Phys.* (in the Press).

RESLER, E. L., JR. & SEARS, W. R. 1958 *J. Aero. Sci.* **25**, 235.

ROTT, N. & CHENG, H. K. 1954 *J. Rat. Mech. Anal.* **3**, 357.

SEARS, W. R. & RESLER, E. L., JR. 1959 *J. Fluid Mech.* **5**, 257.